5-2023

Correlation of Intracellular Metabolites with Optical Metabolic Imaging in Polarized Macrophages as Indicators of Metabolic Reprogramming

Abby Claire Denison
University of Arkansas, Fayetteville

Shelby Bess
University of Arkansas, Fayetteville

Correlation of Intracellular Metabolites with Optical Metabolic Imaging in Polarized Macrophages as Indicators of Metabolic Reprogramming

Abby Denison

Mentor: Timothy Muldoon, M.D., Ph.D.

Contributor: Shelby Bess, Ph.D. Candidate

University of Arkansas

Department of Biomedical Engineering

April 26, 2023

Abstract

Macrophages are a type of immune cell that are characterized by their ability to differentiate into various active phenotypes based on environmental stimuli. They can generally be classified as one of two extremes: inflammatory/M1 or wound-healing/M2. Macrophage populations in vivo, however, are rarely homogenous, and since macrophages play vital roles in the immune response, particularly in the context of the tumor microenvironment (TME), it's important to be able to investigate and understand heterogenous macrophage populations to develop more effective treatments. Recently, autofluorescence imaging such as multiphoton microscopy and fluorescence lifetime imaging microscopy (FLIM) of metabolic cofactors NADH and FAD have been used to determine the phenotypes of induvial macrophages based on their characteristic metabolic profiles. M1s show preferential utilization of glycolysis, whereas M2s more heavily utilize oxidative phosphorylation (OXPHOS). However, concentrations of these cofactors within the cells, while a potential indicator of metabolic shifts, can also be affected by environmental factors, such as temperature, pH, and oxygen availability, to name a few. The goal of this research was to verify that the changes observed using autofluorescence imaging were due to changes in metabolism rather than in environmental factors. This was done by comparing the imaging data to gold-standard extracellular flux assays (Seahorse assays) and characteristic metabolic intermediates (lactate and succinate) for the M1 phenotype. Correlations were then done between each of the 3 imaging methods, the 7 parameters from the Seahorse assays, and the concentrations of the 2 intermediates – 41 correlations total. Of the 41 correlations, 10 were statistically significant ($p < 0.05$), and they linked changes in FLIM to changes in metabolite concentrations and Seahorse parameters. These correlations indicate that autofluorescence imaging is a reliable method of monitoring macrophage metabolism during activation.

Introduction

Macrophages are phagocytic immune cells that play a variety of roles in the body. Unlike other immune cells, macrophages have a highly plastic nature which allows them to assume very different functions depending on their environment. These cells possess a wide range of surface receptors that enable them to recognize surface characteristics of cell debris and pathogens and to respond appropriately [1]. In addition to dead cells and pathogens, exposure to other environmental stimuli, such as cytokines, can cause macrophages to differentiate from a resting phenotype, also known as the M0 phenotype, into an active one, which encompasses a broad spectrum of functionalities ranging from host defense, to wound healing, to immune regulation [2]. Tumor-associated macrophages (TAMs) are different still in that they may express more than one of these functionalities simultaneously or may transition from one phenotype to another [2]. However, even though it is important to acknowledge that these cells are highly plastic and adaptable, measurable differences between macrophages that are close together on this spectrum are subtle and difficult to detect, and as a result, they are generally classified as one of two extremes: pro-inflammatory/M1 or anti-inflammatory/M2 [3].

Macrophages that fall into these categories have well established functions and characteristics. M1, or classically activated macrophages are involved mainly with clearing cell debris and destroying pathogens. Macrophages will commonly polarize to this phenotype in the presence of bacterial products like lipopolysaccharide (LPS) or cytokines secreted by helper T cells such as interferon gamma (IFN-γ) [3]. In response to polarization, M1's will then secrete inflammatory cytokines like tumor necrosis factor alpha (TNF-α) and IL-12 [3]. M2, or alternatively activated macrophages are involved in tissue remodeling and wound healing processes and are commonly activated by the presence of cytokines such as IL-4 and IL-13

secreted by other immune cells [3]. Macrophages that undergo alternative activation usually secrete anti-inflammatory cytokines like IL-10 and transforming growth factor beta (TGF-beta) [2,3]. Studies have also shown differences in the phagocytic capacity of polarized macrophages, with the M2 phenotype displaying a higher phagocytic activity than the M1 phenotype [4].

Metabolic Profiles of Differentiated Macrophages

Besides differences in function and cellular products, recent studies have also revealed distinct metabolic profiles for the different macrophage phenotypes involving differences in energy production, nutrient usage, and metabolites generated [5]. These differences can arise from increased or decreased reliance on specific metabolic processes involved in cellular respiration, like glycolysis or oxidative phosphorylation (OXPHOS), or the utilization of an altered version of these processes by the cells.

Basic cellular respiration has 3 major steps: glycolysis, the tricarboxylic acid cycle (TCA cycle), and OXPHOS. Glycolysis is an anaerobic process by which cells can produce 2 molecules of adenosine triphosphate (ATP) and 2 3-carbon molecules of pyruvate from 1 molecule of glucose. In the presence of oxygen, the 2 molecules of pyruvate are shuttled into the mitochondrial matrix where they are oxidized to produce 2 molecules of acetyl-CoA, which then enter the TCA cycle. When functioning normally, the TCA cycle produces ATP, NADH, $FADH_2$, and CO_2. NADH and $FADH_2$ then become electron donors in the electron transport chain (ETC), where the majority of a cell's ATP is generated, along with water molecules [6]. In anaerobic environments, the pyruvate molecules generated from glycolysis will enter a process known as lactic acid fermentation, where pyruvate is transformed into lactate and NAD+ is regenerated [6].

M1 macrophages have been shown to display a glycolytic metabolic profile [5, 7]. Since there is an increase glycolysis and a decrease in OXPHOS, this promotes an increased production of lactate due to pyruvate entering lactic acid fermentation as well as the TCA cycle [5]. Additionally, M1s presents a major break in the TCA cycle at the conversion of succinate to fumarate. The enzyme that catalyzes this reaction, succinate dehydrogenase (SDH), is inhibited, which leads to the accumulation of succinate inside the cell [5]. In contrast, M2 macrophages have been shown to rely more heavily on mitochondrial metabolism such as OXPHOS and fatty acid oxidation (FAO) than M1s [5, 7]. Measurements of oxygen consumption rate (OCR) and extracellular acidification rate (ECAR) can quantify the mitochondrial activity within cells; an increase in OCR indicates elevated OXPHOS, while an increase in ECAR indicates elevated glycolytic metabolism due to a buildup of lactic acid [8].

Macrophages in the Tumor Microenvironment

In the context of the tumor microenvironment (TME), macrophages can play a vital role in either inhibiting or promoting tumor growth and cancer progression. M1 macrophages tend to be anti-tumor, since they have the ability to phagocytose and lyse cancerous cells as well as secrete inflammatory cytokines and chemokines that promote an increased immune response [9, 10]. However, most tumor-associated macrophages (TAMs), which account for the largest population of immune cells in a tumor, assume the M2 phenotype [7, 9]. This is partially due to the rapid growth of tumors resulting in hypoxic regions within them, in which inflammatory molecules like IL-4 and IL-10 are produced. This leads to the recruitment of macrophages to the site and their polarization to the M2 phenotype [9]. Additionally, since cancer cells tend to rely on glycolysis and consume most of the available glucose, TAMs will naturally shift towards OXPHOS and FAO to meet their energy demands, which is consistent with the M2 metabolic

profile [7]. In this context, the M2 phenotype adopted by most TAMs encourages tumor growth and metastasis by promoting angiogenesis and secreting growth factors such as TGF-β and VEGF, as well as suppressing an innate immune response [9, 10].

Methods of Evaluating Heterogenous Macrophage Populations

Although most TAMs assume the M2 phenotype, the macrophage populations within and around tumors are far from homogenous, displaying multiple phenotypes and functionalities, of which M1 and M2 are the most well defined and understood [11]. This level of heterogeneity within the tumor can make developing effective treatments very difficult, resulting in the need to be able to monitor macrophage function at the cellular level within the TME [11]. Previous methods of evaluating macrophage function were limited to population-level, destructive assays such as ELISAs, flow cytometry, and PET/MRI imaging [11]. While these methods are useful for qualitatively determining the characteristics of macrophage populations as a whole, they are unable to provide any spatial or temporal information about the functionality of the cells.

Recent advances in cellular imaging techniques have utilized autofluorescence imaging methods, such as fluorescent lifetime and multiphoton imaging, to observe metabolic changes at the cellular level, and since cellular metabolism has been correlated to cellular function, this type of imaging can provide insight into the functionality of the cells as well [11]. Using this type of imaging to observe cellular metabolic changes in real time relies on the autofluorescence properties of NADH and FAD, both of which are metabolic cofactors that play important roles in OXPHOS and/or glycolysis [12]. The fluorescent intensities of NADH and FAD can be measured using multiphoton microscopy and used to determine the intracellular concentrations of each of these cofactors, which provides information about the oxidation-reduction state of the cell [11]. Since FAD is only involved in OXPHOS, while NADH is involved in both OXPHOS

and glycolysis, the ratio of FAD/NADH+FAD, also known as the redox ratio, can be used to determine the metabolic preference of the cell [12]. An increase in the redox ratio indicates an increase in OXPHOS and/or a decrease in glycolysis, and vice versa. However, since the autofluorescence of these molecules is very faint and can be scattered through tissue, an alternative method of imaging called fluorescent lifetime imaging microscopy (FLIM) can be used to overcome this limitation [13].

FLIM can be used to quantitatively determine the amounts of free NADH, which has a shorter fluorescent lifetime, and protein-bound NADH, which has a longer fluorescent lifetime [13, 14]. Data acquired via FLIM can reveal both the mean fluorescent lifetime of NADH as well as the ratio of free to protein-bound NADH, also called the A1/A2 ratio, at the cellular level [13]. Glycolysis involves more free NADH, whereas OXPHOS involves more protein-bound NADH. Therefore, it can generally be said that a metabolic shift towards glycolysis and away from OXPHOS will result in a decrease in the mean NADH lifetime and an increase in the A1/A2 ratio [13]. Autofluorescence imaging of NADH and FAD have been used in previous studies to monitor macrophage metabolism across 3D space and time, to provide a better understanding of their function in the TME [11].

While these autofluorescence imaging methods are a convenient, label-free, and non-invasive method of monitoring cellular metabolic activity, they are not without their limitations. NADH and FAD are established biomarkers for the cellular redox state and metabolism, but their intracellular concentrations and fluorescent lifetimes can be affected by factors other than changes in metabolism [12, 14]. For example, NAD+, which does not exhibit autofluorescence, can act as a regulatory molecule that affects the fluorescent lifetime of protein-bound FAD [13, 14]. Generally speaking, the fluorescent lifetimes of free NADH and FAD can also be impacted

by changes in oxygen availability, concentrations of certain amino acids, temperature, and pH of the cellular environment [14]. This emphasizes the need to confirm that changes in the optical redox ratio, mean lifetime, and A1/A2 ratio are due to metabolic changes within the cell rather than changes in the cellular environment.

The goal of this research is to validate these methods of autofluorescence imaging as a reliable way of detecting changes in cellular metabolism by establishing correlations with concentration of intermediates characteristic to known macrophage metabolic profiles and gold-standard metabolic assays that evaluate mitochondrial function.

Objectives

The objectives of this project are to:

1. Quantify intracellular succinate and lactate concentrations in M0 and M1 macrophages at 4 different time points in the differentiation process using colorimetric assays.
2. Quantify the OCR and ECAR in M0 and M1 macrophages at 4 different timepoints in the differentiation process using a Seahorse assay.
3. Determine if there are any significant correlations between the metabolites, Seahorse metrics, and/or imaging data to validate the autofluorescence imaging methods as tools to evaluate cellular metabolism.

Materials and Methods

Macrophage Culture

Murine RAW 264.7 macrophages were maintained in Roswell Park Memorial Institute (RPMI)-1640 medium supplemented with 10% fetal bovine serum (FBS) and 1% gentamicin.

The macrophages were then seeded in a 35 mm MatTek dish for fluorescent imaging at a density of 1 x 10^6 cells/mL and allowed to incubate for 24 hours to allow for cell adhesion. After this initial 24-hour period, macrophage activation was stimulated with either 10 ng/mL of IFN-γ (M1 polarization) or no cytokine supplementation (M0) and incubated for an additional 24 to 72 hours.

Autofluorescence Imaging

Prior to imaging, cells were moved to a microincubator with controllable temperature and humidified gas delivery of 5% CO_2. A custom inverted multiphoton imaging system (Bruker custom system) was used to capture images. NAD(P)H fluorescence was captured with a 460 (± 20) nm band pass filter with 755 nm excitation; FAD fluorescence was captured with a 525 (± 25) nm band pass filter with 855 nm excitation. An integrated FLIM module was used to measure mitochondrial function with respect to the different components contributing to NADH fluorescence. Images were taken starting 24 hours after cell seeding (0 hours), and at 24-hour intervals following cytokine stimulation (24, 48, and 72 hours) for both M0 and M1 macrophages.

Metabolic Intermediate Detection Assays

Succinate and lactate are important intermediates that are associated with increased glycolytic metabolism. In order to quantify the presence and concentration of succinate in M0 and M1 macrophages at multiple timepoints during differentiation, a colorimetric assay was used. First, a standard curve was prepared using a 1 mM succinate standard. Once the cells were cultured and differentiated, they were harvested at 4 different timepoints following cytokine stimulation: 0 hours (immediately following cytokine stimulation), 24 hours, 48 hours, and 72

hours. The cells were harvested at a density of 1 x 10^6 cells using Accutase. They were then washed with PBS, resuspended in ice-cold Succinate Assay Buffer, and centrifuged. The supernatant was collected using a 10 kDa spin column and kept on ice until the start of the assay. In addition to the standard wells, the sample wells were then prepared in triplicate for each timepoint according to the protocol in a 96-well plate, which was transferred to a microplate reader and read at OD = 450 nm. The succinate concentrations for the two experimental groups (M0 and M1) for each timepoint (0, 24, 48, and 72 hours) were calculated using the following equation: $Succinate\ (mM) = \frac{A}{B} * D$, where A is the amount of succinate calculated using the standard curve (average of the triplicate values for each culture condition), B is the sample volume added to each reaction well (µL), and D is the dilution factor.

A colorimetric assay was also used to confirm the presence and concentration of lactate in M0 and M1 macrophages. First, a standard curve was prepared using a 1 mM lactate standard. Once the cells were cultured and differentiated, cells were harvested at the same 4 timepoints following cytokine stimulation as for the succinate assay described above. Cells were harvested at a density of 2 x 10^6 cells using Accutase. The cells were then washed with PBS, resuspended in the lactate assay buffer, and centrifuged. The supernatant was collected, transferred to a microcentrifuge tube, and kept on ice. Here, an additional step was performed to remove any endogenous lactate dehydrogenase (LDH) in the samples that could degrade lactate by using a Deproteinizing Sample Preparation Kit – TCA. Once the sample had been deproteinized, the standard wells were prepared in a 96-well plate along with samples wells which were prepared in triplicate for each timepoint. The plate was transferred to a microplate reader and read at OD = 450 nm. The lactate concentrations for the two experimental groups (M0 and M1) at each timepoint (0, 24, 48, and 72 hours) were calculated using the following equation:

$Lactate\ (mM) = \frac{La}{Sv} * D$, where La is the amount of lactate calculated using the standard curve (average of the triplicate values for each culture condition), Sv is the sample volume added to each reaction well (µL), and D is the dilution factor.

Oxygen Consumption Rate

A Seahorse XFp extracellular flux analyzer was used to measure the OCR. Cells were plated in the Seahorse 8-well miniplate, and cell densities were optimized to ensure that cells were not over-confluent after cytokine stimulation. After cytokine stimulation, the cell-media was replaced with Seahorse assay media and placed in a non-CO_2 incubator at 37°C for 1 hour prior to the start of the assay. During the assay, 3 compounds were added sequentially to disrupt specific parts of the ETC: oligomycin (1.5 µM), carbonyl cyanide p-triflouromethoxyphenylhydrazone (FCCP, 1 µM), and rotenone/antimycin A (Rot/AA, 1 µM). By targeting different elements of mitochondrial respiration, this assay is able to provide information about the OCR and ECAR, as well as about 7 other key parameters derived from OCR: basal respiration, ATP-linked respiration, proton production rate (PPR)/H+ proton leak, spare respiratory capacity, maximal respiration, non-mitochondrial respiration, and coupling efficiency [15]. More thorough descriptions of the injection compounds, their effects on the electron transport chain, and calculations of key parameters are provided in ***Appendix 1***.

Results

Autofluorescence Imaging

Measurements of redox ratio, NADH lifetime, and A1/A2 ratio were obtained from monolayer cultures of RAW 264.7 macrophages at 4 timepoints (0, 24, 48, and 72 hours) following cytokine stimulation. Results are shown below in ***Figure 1.***

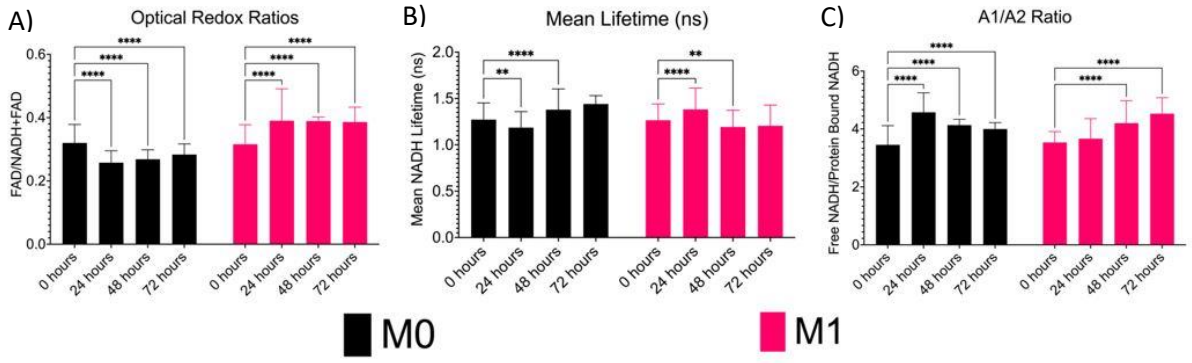

Figure 1: *For both M0 and M1 macrophages, changes in A) optical redox ratio, B) mean NADH lifetime, and C) A1/A2 ratio over time. **p ≤ 0.01, ****p ≤ 0.0001*

As seen in ***Figure 1A***, the M0 macrophages showed a significant decrease ($p < 0.0001$) in redox ratio from 0.32 to 0.258 after 24 hours, and then a steady increase over the next 2 timepoints. The M1s showed a significant increase ($p < 0.0001$) in redox ratio from 0.316 to 0.390 after 24 hours, and then maintained a constant redox ratio of around 0.386 for both the 48- and 72-hour timepoints. As previously mentioned, FLIM tends to be more sensitive than redox imaging since it isn't intensity-based and prone to interference from scattering [14]. FLIM provides information regarding the mean lifetime of NADH and the relative amounts of free vs protein-bound NADH, also called the A1/A2 ratio, results for which are shown in ***Figure 1B*** and ***Figure 1C***, respectively. As seen in ***Figure 1B***, M0 macrophages show a significant decrease of 0.086 ns in mean NADH lifetime at 24 hours ($p = 0.0012$) and then an increase at 48 hours ($p <$

0.0001). M1 macrophages showed a significant increase in mean NADH lifetime of 0.117 ns at 24 hours ($p < 0.0001$) followed by a return to initial mean lifetime of around 1.206 ns after 72 hours.

Mean NADH lifetime data can be further analyzed using a biexponential decay model to separate the short (A1) and long (A2) lifetime components which are representative of free and protein-bound NADH, respectively [16]. The results of this analysis are shown in ***Figure 1C***. The M0 macrophages showed a significant increase from 3.452 to 4.576 in A1/A2 ratio after 24 hours ($p < 0.0001$) followed by a steady decrease over the 48- and 72- hour timepoints. M1 macrophages showed a steady increase in A1/A2 ratio over all 4 timepoints, but not reaching a significant increase ($p < 0.0001$) until 48 hours post-cytokine stimulation. Overall, the trends indicate that M0s show an initial spike in glycolytic metabolism and then shift towards OXPHOS over time, whereas M1s show an initial spike in mitochondrial respiration and then shift towards glycolytic metabolism over time.

Metabolic Intermediates

Results displaying the concentrations of intracellular lactate and succinate are shown below in ***Figure 2***. A one-way ANOVA was used to determine significant differences and a Tukey's multiple comparisons test were used to determine statistically significant differences

between experimental groups, and a Tukey's honestly significant difference (HSD) test was used in post-hoc analysis [16].

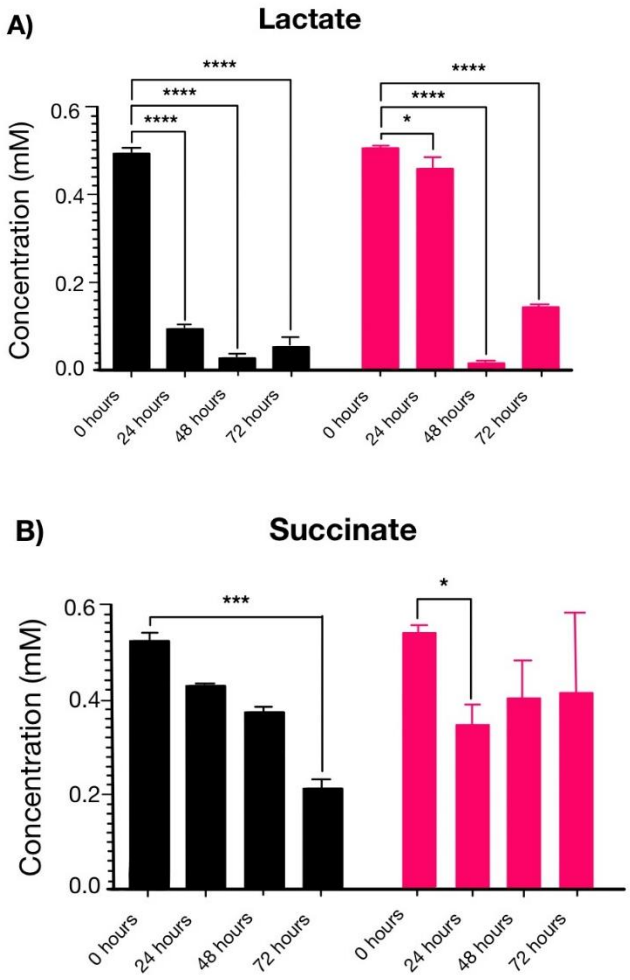

Figure 2: *Intracellular concentrations of A) lactate and B) succinate for M0 and M1 macrophages. *p ≤ 0.05, **p ≤ 0.01, ***p ≤ 0.001, ****p ≤ 0.0001*

As seen in ***Figure 1A***, the M0 macrophages show a significant decrease ($p < 0.0001$) in lactate at 24 hours and then remains relatively consistent for the 48- and 72- hour timepoints. The M1 macrophages show a slight decrease in lactate concentration at 24 hours, then a dramatic decrease at 48 hours ($p < 0.0001$), followed by a slight increase at 72 hours. As seen in ***Figure 2B***, the M0s show a consistent decrease in succinate concentration across all 4 timepoints, whereas the M1s show an initial decrease ($p < 0.05$) in succinate concentration at 24 hours,

followed by a slight increase over the 48- and 72- hour timepoints. Overall, the trends seen in succinate concentration correspond to some of the trends seen in the autofluorescence imaging data. They indicate that the M0s become more aerobic over time, while M1s show an initial switch to mitochondrial respiration and then a gradual shift towards glycolysis over time.

Oxygen Consumption Rate and Associated Parameters

The results from the Seahorse XFp extracellular flux analyzer included the OCR and ECAR, as well as many other parameters that were derived from them. Cells for each experimental group (M0 and M1) were plated in triplicate for each timepoint; the averages of these triplicates were used to calculate the numerical values for the OCR, ECAR, and other associated parameters for each group. There were 7 OCR parameters that were obtained from the Seahorse data: non-mitochondrial respiration, basal respiration, maximal respiration, H+ proton leak, ATP production, coupling efficiency, and spare respiratory capacity. Additionally, the OCR and ECAR were used to categorize the macrophages at each timepoint as 1 of 4 energetic phenotypes, shown in ***Figure 3D***.

As seen in ***Figure 3A*** and ***Figure 3B***, both M0 and M1 macrophages followed similar trends in OCR and ECAR. They both experienced a large jump in OCR at 24 hours post-cytokine stimulation, followed by a small decrease at 48 and 72 hours, although the M1s experienced a greater decrease than the M0s. The M0s showed a steady increase in ECAR across the 24- and 48- hour timepoints, followed by a decrease after 72 hours. The M1s showed a significant increase in ECAR after 24 hours, followed by a slight increase at 48 hours and a decrease at 72 hours. Both M0 and M1 macrophages also followed similar trends in all 7 OCR parameters. Although, the M1s displayed a higher maximal respiration, H+ proton leak, and spare respiratory capacity than M0s at the 24- and 48- hour timepoints.

Additionally, there are 4 main energy phenotypes that a cell can display: quiescent, aerobic, glycolytic, and energetic. These states are determined by comparing the OCR to ECAR. The quiescent state corresponds to low OCR and ECAR, whereas the aerobic state corresponds to high OCR and ECAR. An aerobic energy phenotype corresponds to high OCR and low ECAR, and the glycolytic state corresponds to low OCR and high ECAR [17]. Initially, both M0s and M1s displayed a quiescent energy profile. After 24 hours, the M0s were aerobic while the M1s were energetic. At 48 hours, both M0s and M1s were energetic. Finally, at 72 hours, the M0s were aerobic and, interestingly, the M1s were on the border between aerobic and quiescent.

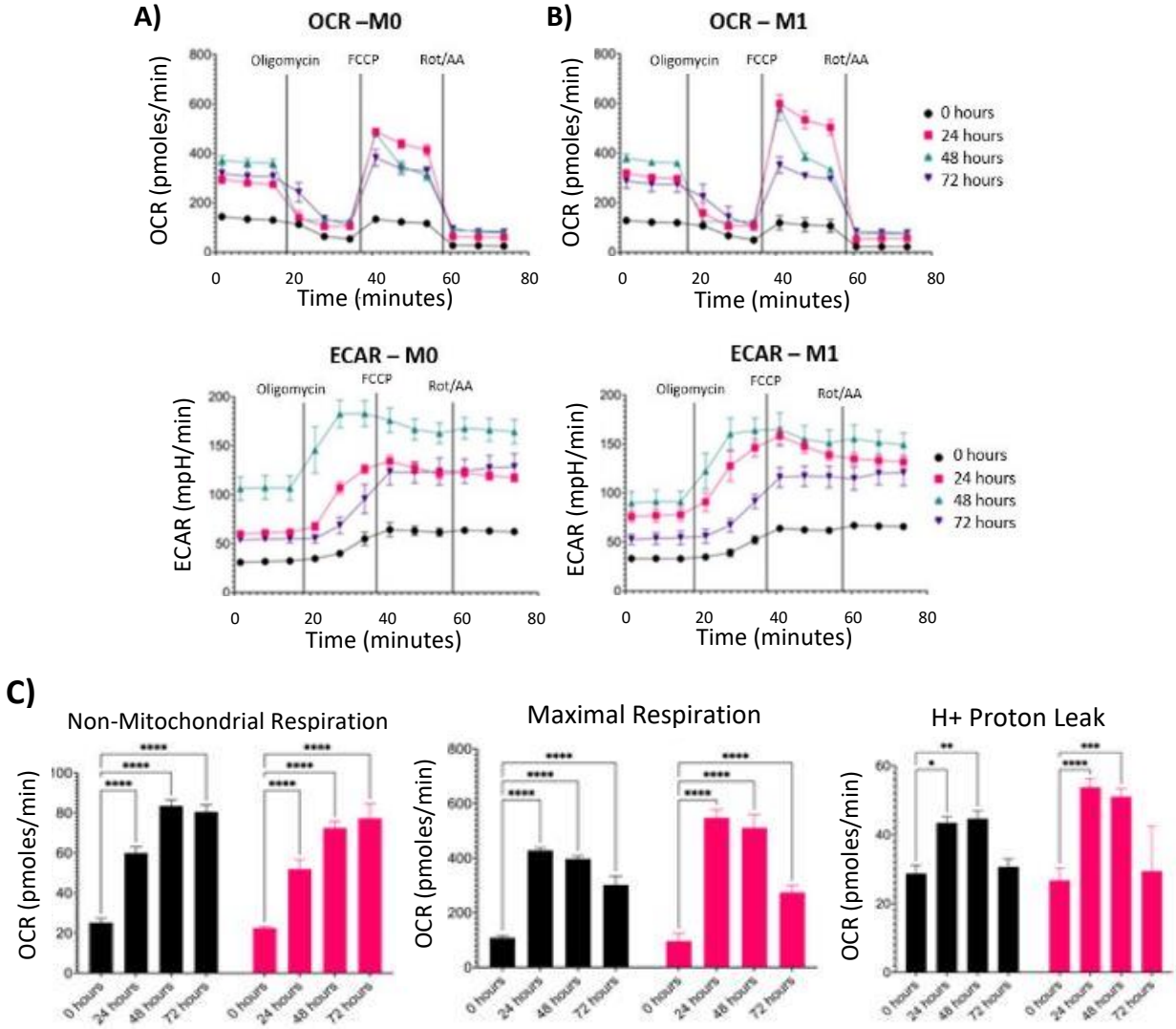

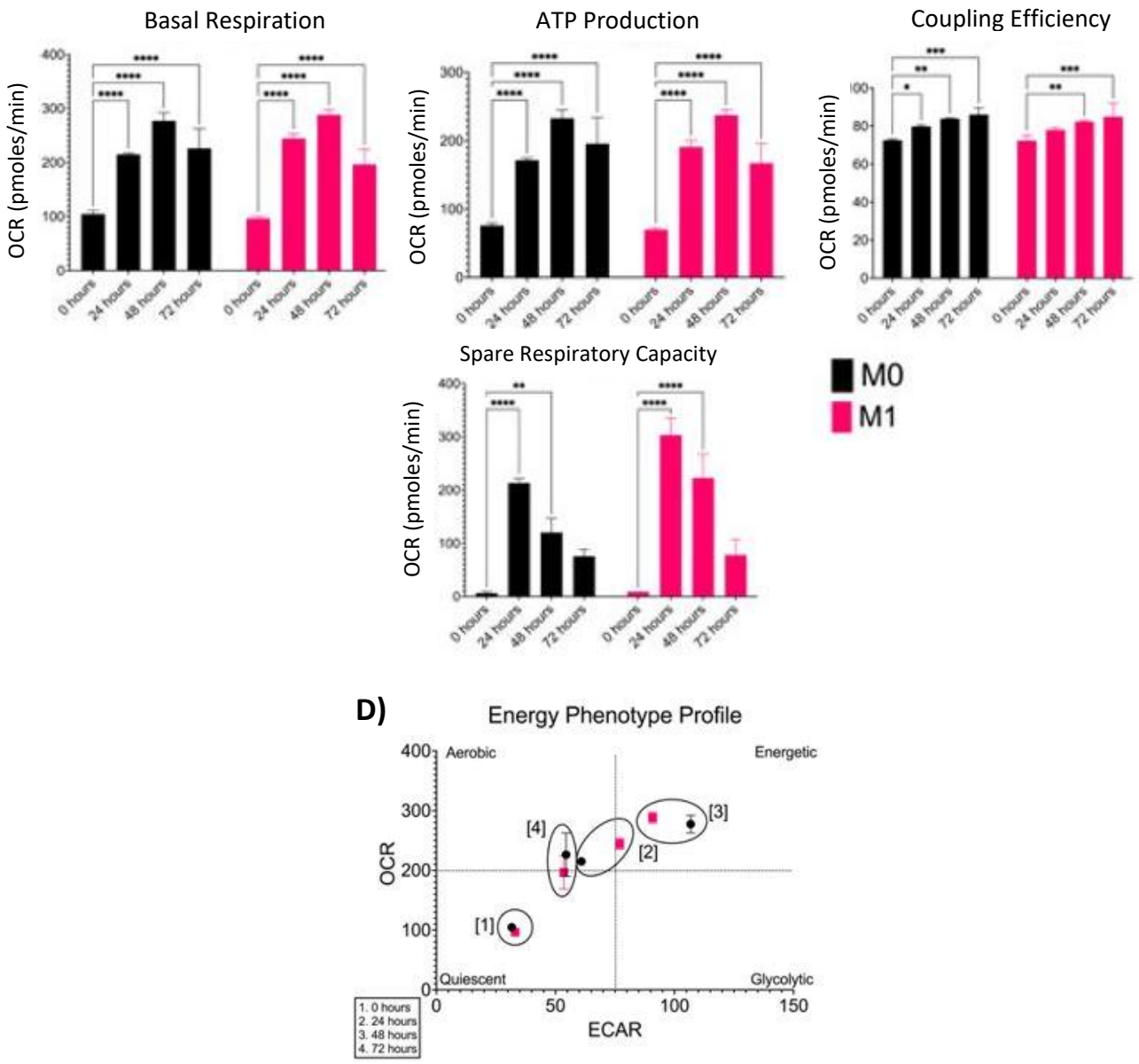

Figure 3: *OCR and ECAR profiles for A) M0 and B) M1 macrophages, C) Values for key OCR parameters, D) Energy phenotypes for M0 and M1 macrophages at all timepoints. *p ≤ 0.05, **p ≤ 0.01, ***p ≤ 0.001, ****p ≤ 0.0001*

Correlational Analysis

Correlational plots were used to compare the autofluorescence imaging data (redox ratio, mean NADH lifetime, and A1/A2 ratio) to both the metabolic intermediate data (lactate and succinate concentration) and the XF assay data (OCR parameters. For each comparison, the

Pearson's R-value and the p-value were calculated to determine the strength of the correlation. 41 comparisons were made overall, 10 of which were found to be statistically significant. First, each of the metabolic intermediates were compared to the 7 key OCR parameters. Lactate concentration was found to significantly correlate with non-mitochondrial respiration ($p = 0.002$, $r = -0.9047$), basal respiration ($p = 0.0307$, $r = -0.7539$), ATP production ($p = 0.0163$, $r = -0.8033$), and coupling efficiency ($p = 0.0039$, $r = -0.8805$). Succinate concentration was found to significantly correlate with non-mitochondrial respiration ($p = 0.0273$, $r = -0.7641$), ATP production ($p = 0.0434$, $r = -0.7213$), and coupling efficiency ($p = 0.0183$, $r = -0.7952$).

Each of the autofluorescence imaging methods were then compared to each of the OCR parameters. Neither the optical redox ratio nor the mean NADH lifetime had any significant correlations with the OCR parameters. However, the A1/A2 ratio showed a correlation with non-mitochondrial respiration ($p = 0.0354$, $r = 0.7410$) and coupling efficiency ($p = 0.0394$, $r = 0.7311$). Lastly, each of the autofluorescence imaging methods were compared to each of the metabolic intermediates. Only one significant correlation was observed between the A1/A2 ratio and lactate concentration ($p = 0.0133$, $r = -0.8171$). Significant correlations are shown below in ***Figure 4***. Overall, this demonstrates that there are multiple significant correlations between the autofluorescence imaging methods and the more standard metabolic assays.

A)

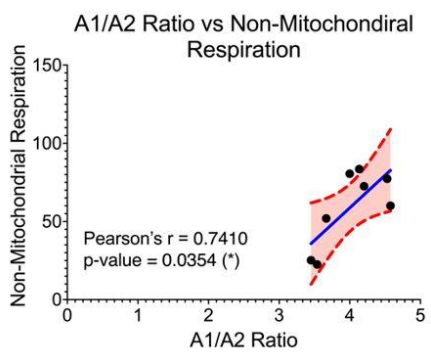
A1/A2 Ratio vs Non-Mitochondiral Respiration
Non-Mitochondrial Respiration
A1/A2 Ratio
Pearson's r = 0.7410
p-value = 0.0354 (*)

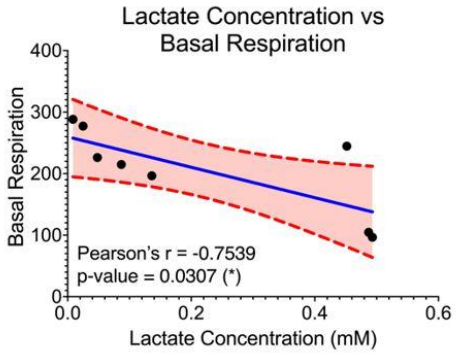
Lactate Concentration vs Basal Respiration
Basal Respiration
Lactate Concentration (mM)
Pearson's r = -0.7539
p-value = 0.0307 (*)

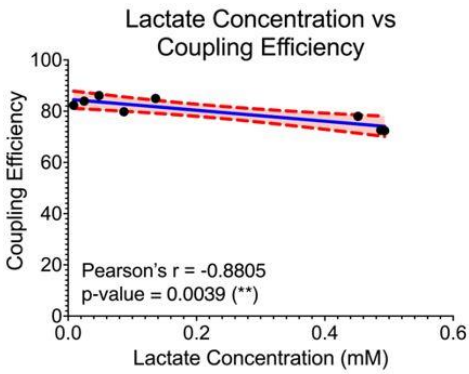
Lactate Concentration vs Coupling Efficiency
Coupling Efficiency
Lactate Concentration (mM)
Pearson's r = -0.8805
p-value = 0.0039 (**)

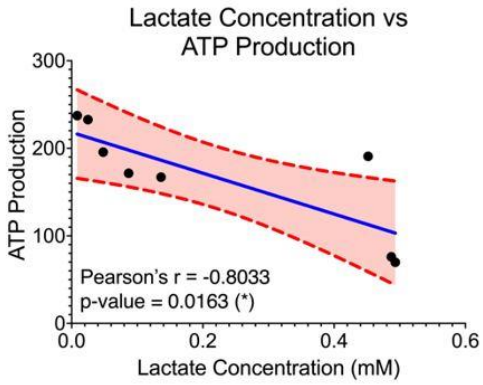
Lactate Concentration vs ATP Production
ATP Production
Lactate Concentration (mM)
Pearson's r = -0.8033
p-value = 0.0163 (*)

B)

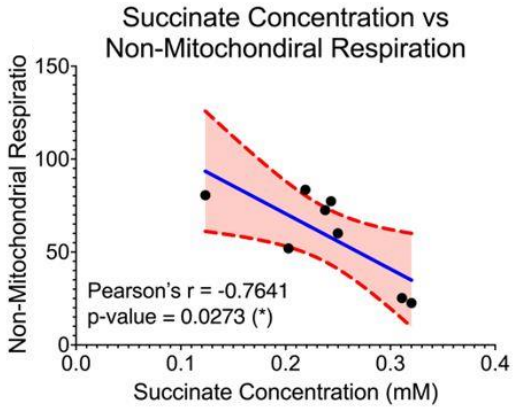
Succinate Concentration vs Non-Mitochondiral Respiration
Non-Mitochondrial Respiratio
Succinate Concentration (mM)
Pearson's r = -0.7641
p-value = 0.0273 (*)

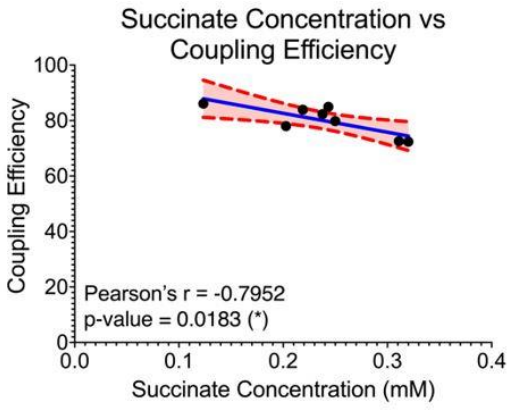
Succinate Concentration vs Coupling Efficiency
Coupling Efficiency
Succinate Concentration (mM)
Pearson's r = -0.7952
p-value = 0.0183 (*)

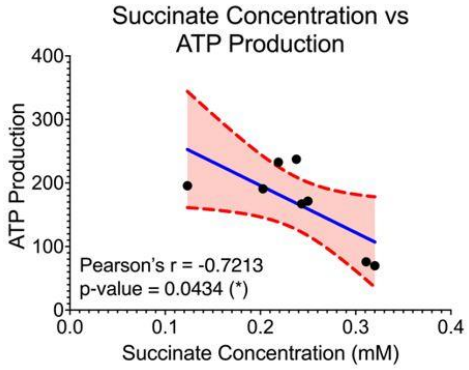
Succinate Concentration vs ATP Production
ATP Production
Succinate Concentration (mM)
Pearson's r = -0.7213
p-value = 0.0434 (*)

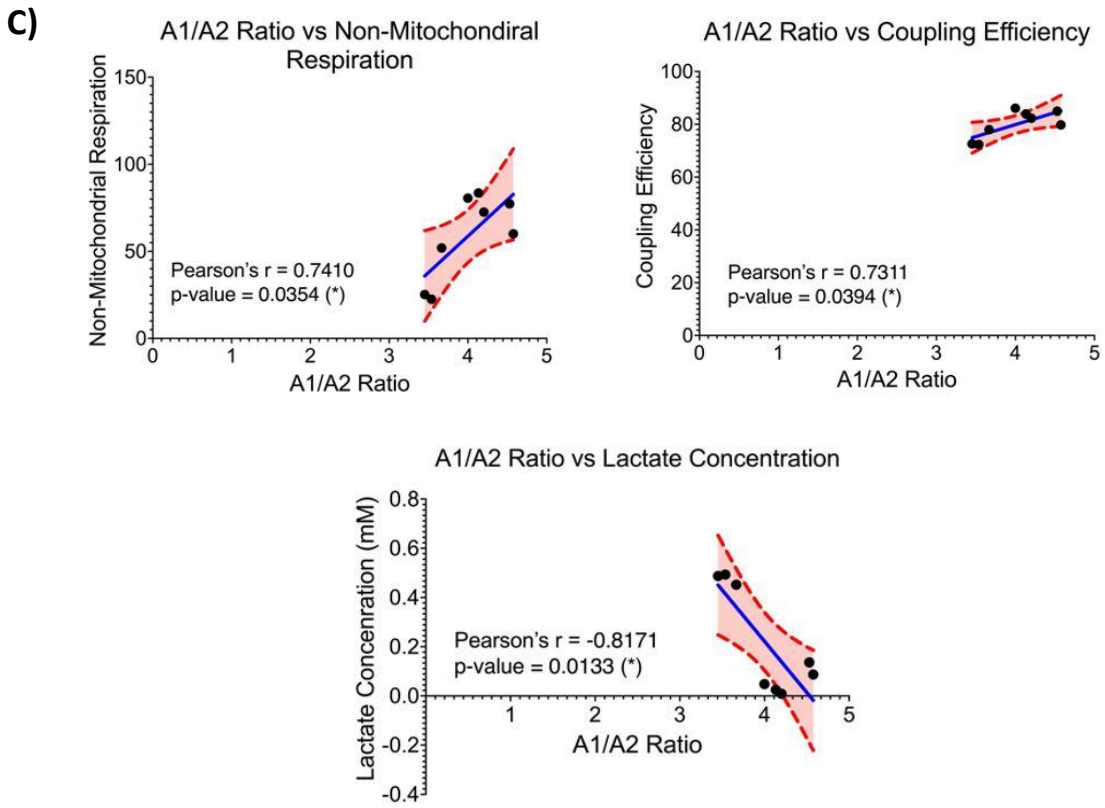

Figure 4: *Significant correlations between A) Lactate and key OCR parameters, B) Succinate and key OCR parameters, C) Autofluorescence imaging methods and key OCR parameters, D) Autofluorescence imaging and metabolic intermediates. *p ≤ 0.05, **p ≤ 0.01; linear regression line (blue) and 95% confidence intervals (red)*

Discussion

Significant Correlations Between Metabolites and OCR Parameters

The analysis of cellular energetics is essential for a thorough understanding of cell physiology and pathophysiology and has led to advances in monitoring cellular metabolism [18]. An extracellular flux (XF) assay has become the gold-standard for measuring bioenergetics and mitochondrial function because it's both non-destructive and label-free [19]. Measuring changes in XF, which is oxygen and proton concentrations in the cell media, provides insight into the aerobic and glycolytic activity of the cells [19]. However, these XF systems are complex and

expensive, so this experiment sought to validate whether either of the metabolic intermediates (lactate or succinate) could potentially be used as simple biomarkers to indicate a shift towards glycolytic metabolism.

The results showed 4 significant correlations between lactate concentration and OCR parameters, and 3 significant correlations between succinate concentration and OCR parameters. The lactate correlations with non-mitochondrial respiration and coupling efficiency were the most significant ($p < 0.01$). Since lactate and succinate had relatively similar correlations, it is likely that they are both indicative of metabolic changes within the cell. Also, since they both had the same types of linear relationships (positive or negative) with the same OCR parameters, it follows that an increase in both of these metabolites is indicative of the same type of metabolic shift, either towards or away from glycolysis.

Both the lactate and succinate correlations with non-mitochondrial metabolism and coupling efficiency showed inverse relationships, meaning that as one factor increased, the other decreased. In this case, an increase in lactate and succinate corresponded to a decrease in non-mitochondrial respiration, coupling efficiency, and ATP production. Coupling efficiency is the fraction of mitochondrial respiration that is being used to generate ATP [20]. As lactate and succinate concentrations increase in correspondence with increased glycolysis, the cell's reliance on OXPHOS to produce ATP decreases [21]. Since the cells are less reliant on OXPHOS for ATP production, it could be that the fraction of mitochondrial respiration being used to generate ATP relative to the basal rate of respiration decreases, which in turn results in a decrease in coupling efficiency. At a high coupling efficiency, most of the mitochondrial respiration is being used to generate ATP. However, when the mitochondrion is not actively producing ATP, it is an

important source of reactive oxygen species (ROS) production [22]. The upregulation of mitochondrial ROS production in M1 macrophages may support this correlation [21].

Additionally, the process of glycolysis yields 2 net ATP, whereas the TCA cycle yields 36 net ATP, making glycolysis an inefficient method of metabolism in terms of ATP production [23]. However, in M1 macrophages, glycolysis is often preferentially used even in the presence of oxygen because it can be activated rapidly and used sustain other cellular functions such as phagocytosis and the secretion of inflammatory cytokines [23]. The correlation between an increase in lactate and succinate and a decrease in ATP production indicates that as macrophages shift towards glycolysis, their mitochondrial ATP production decreases. This supports the conclusion that M1 macrophages have a greater reliance on glycolysis to meet their energy demands and sustain immune functions, even though it's relatively inefficient.

Significant Correlations Indicate that FLIM Can Accurately Report Metabolic Changes

When the autofluorescence imaging methods were compared to both the intermediate concentrations and the OCR parameters, 3 significant correlations were observed. An increase in the A1/A2 ratio corresponded to an increase in non-mitochondrial respiration, an increase in coupling efficiency, and a decrease in lactate. The positive relationship between the A1/A2 ratio and the 2 OCR parameters is supported by the negative relationship between lactate concentration and those same 2 OCR parameters. It can be said then that lactate, A1/A2 ratio, coupling efficiency, and non-mitochondrial respiration all showed strong correlations with each other that link FLIM imaging to both the metabolic intermediate lactate and the gold-standard Seahorse assay. This indicates that FLIM is capable of accurately reporting changes in cellular metabolism.

Also worth mentioning is the correlation between succinate and NADH lifetime, which was almost significant ($p = 0.0865$). It is known that an increase in succinate and a decrease in NADH lifetime both signify a glycolytic shift [5,13]. Therefore, it could be said, based on this correlation, that a decrease in mean NADH lifetime could be an indicator of glycolysis. Overall, the results of this study show that significant correlations exist between gold-standard metabolic assays and the results of newer autofluorescence imaging methods. FLIM and multiphoton imaging have shown to be able to reliably monitor metabolic changes in macrophages during activation and could be used as tools in the future to observe changes in cellular metabolism and associated function in other types of immune cells during activation as well.

References

1. Kolliniati O, Ieronymaki E, Vergadi E, Tsatsanis C. Metabolic regulation of MacrophageActivation. Journal of Innate Immunity. 2021;14(1):51–68.
2. Mosser DM, Edwards JP. Exploring the full spectrum of macrophage activation. Nature Reviews Immunology. 2008;8(12):958–69.
3. Viola A, Munari F, Sánchez-Rodríguez R, Scolaro T, Castegna A. The metabolic signature of macrophage responses. Frontiers in Immunology. 2019;10.
4. Jaggi U, Yang M, Matundan HH, Hirose S, Shah PK, Sharifi BG, et al. Increased phagocytosis in the presence of enhanced M2-like macrophage responses correlates with increased primary and latent HSV-1 infection. PLOS Pathogens. 2020;16(10).
5. Wculek SK, Dunphy G, Heras-Murillo I, Mastrangelo A, Sancho D. Metabolism of tissue macrophages in homeostasis and pathology. Cellular & Molecular Immunology. 2021;19(3):384–408.
6. Bartee DL, Brook J. An overview of cellular respiration [Internet]. MHCC Biology 112 Biology for Health Professions. OpenOregon Educational Resources; 2019 [cited 2023Apr18]. Available from: https://openoregon.pressbooks.pub/mhccbiology112/chapter/an-overview-of-cellular-respiration/.
7. Zhang Q, Wang J, Yadav DK, Bai X, Liang T. Glucose metabolism: The metabolic signature of Tumor Associated Macrophage. Frontiers in Immunology. 2021;12.
8. Plitzko B, Loesgen S. Measurement of oxygen consumption rate (OCR) and extracellular acidification rate (ECAR) in culture cells for assessment of the energy metabolism. BIO-PROTOCOL. 2018;8(10).
9. Liu J, Geng X, Hou J, Wu G. New insights into M1/M2 macrophages: Key modulators in cancer progression. Cancer Cell International. 2021;21(1).
10. Anderson NR, Minutolo NG, Gill S, Klichinsky M. Macrophage-based approaches for cancer immunotherapy. Cancer Research. 2021;81(5):1201–8.
11. Heaster TM, Humayun M, Yu J, Beebe DJ, Skala MC. Autofluorescence imaging of 3D tumor–macrophage microscale cultures resolves spatial and temporal dynamics of macrophage metabolism. Cancer Research. 2020;80(23):5408–23.
12. Heikal AA. Intracellular coenzymes as natural biomarkers for metabolic activities and mitochondrial anomalies. Biomarkers in Medicine. 2010;4(2):241–63.
13. Schaefer PM, Kalinina S, Rueck A, von Arnim CAF, von Einem B. NADH autofluorescence-A marker on its way to boost Bioenergetic Research. Cytometry Part A. 2018;95(1):34–46.
14. Skala MC, Riching KM, Gendron-Fitzpatrick A, Eickhoff J, Eliceiri KW, White JG, et al. In vivo multiphoton microscopy of NADH and fad redox states, fluorescence lifetimes, and cellular morphology in precancerous epithelia. Proceedings of the National Academy of Sciences. 2007;104(49):19494–9.
15. Seahorse XFp cell mito stress test kit user guide - agilent technologies [Internet]. Agilent. Agilent Technologies Inc.; 2019 [cited 2023Apr18]. Available from:

https://www.agilent.com/cs/library/usermanuals/public/XFp_Cell_Mito_Stress_Test_Kit_User_Guide.pdf.
16. Jones JD, Ramser HE, Woessner AE, Veves A, Quinn KP. Quantifying age-related changes in skin wound metabolism using in vivo multiphoton microscopy. Advances in Wound Care. 2020;9(3):90–102.
17. Dier U, Shin D-H, Hemachandra LP, Uusitalo LM, Hempel N. Bioenergetic analysis of ovarian cancer cell lines: Profiling of histological subtypes and identification of a mitochondria-defective cell line. PLoS ONE. 2014;9(5).
18. Grey JFE, Townley AR, Everitt NM, Campbell-Ritchie A, Wheatley SP. A cost-effective, analytical method for measuring metabolic load of mitochondria. Metabolism Open. 2019;4:100020.
19. Ferrick DA, Neilson A, Beeson C. Advances in measuring cellular bioenergetics using extracellular flux. Drug Discovery Today. 2008;13(5-6):268–74.
20. Schmidt CA, Fisher-Wellman KH, Neufer PD. From OCR and ECAR to energy: Perspectives on the design and interpretation of Bioenergetics Studies. Journal of Biological Chemistry. 2021;297(4):101140.
21. Kelly B, O'Neill LAJ. Metabolic reprogramming in macrophages and dendritic cells in innate immunity. Cell Research. 2015;25(7):771–84.
22. Murphy MP. How mitochondria produce reactive oxygen species. Biochemical Journal. 2008;417(1):1–13.
23. Liu Y, Xu R, Gu H, Zhang E, Qu J, Cao W, et al. Metabolic reprogramming in macrophage responses. Biomarker Research. 2021;9(1).

Appendix 1: Definitions and Calculations of Parameters for Mitochondrial Function from OCR Curve

Oligomycin is the first compound injected during the Seahorse assay, and it inhibits ATP Synthase, also known as complex V in the ETC, which catalyzes the production of ATP from ADP and phosphate. This causes a decrease in OCR which is specifically linked to and can be used to calculate ATP production [15]. FCCP is the second compound injected, and it disrupts the mitochondrial membrane potential, which allows electrons to flow freely through the ETC through complex IV. This section of the curve can be used to calculate spare respiratory capacity [15]. Rot/AA is the third sequential injection, and it inhibits both complex I and complex III, which, at this point, completely inhibits mitochondrial respiration. This allows for the calculation of any respiration that is taking place outside of the mitochondria [15]. The following definitions (except for coupling efficiency) are taken from the Seahorse XFp Cell Mito Stress Test User Guide [15].

- Basal Respiration: Oxygen consumption used to meet cellular ATP demand resulting from mitochondrial proton leak. This shows the energetic demand of the cell under baseline conditions.
- ATP-Linked Respiration/ATP Production: The decrease in OCR following the first injection (oligomycin) that represents the portion of basal respiration that was being used to drive ATP production.
- H+ Proton Leak: Remaining basal respiration that is not coupled to ATP production.
- Maximal Respiration: the maximum OCR reached after the second injection (FCCP). This shows the maximum rate of respiration that the cell can achieve.

- Spare Respiratory Capacity: This is defined as the difference between maximal respiration and basal respiration. It indicates the cell's ability to respond to increased energy demand under stress.
- Non-mitochondrial Respiration: Oxygen consumption that persists independently of the mitochondria after the third injection (Rot/AA).
- Coupling Efficiency: This is defined as the proportion of mitochondrial respiratory rate that is used to drive ATP synthesis in any particular condition [19].

Acknowledgements

This material is based on work supported by the National Institutes of Health (1R15CA202662-01), National Science Foundation (CBET 1751554) and the Arkansas Biosciences Institute. *Any opinions, findings, and conclusions or recommendations expressed in this material are those of the authors and do not necessarily reflect the views of the acknowledged funding agencies.* **This research has been supported by an Honors College Research Grant.**